Pressure-Induced Ferromagnetism due to an Anisotropic Electronic Topological Transition in $Fe_{1.08}Te$

K. Mydeen,[1] D. Kasinathan,[1] C. Koz,[1] S. Rößler,[1] U. K. Rößler,[2] M. Hanfland,[3] A. A. Tsirlin,[4] U. Schwarz,[1] S. Wirth,[1] H. Rosner,[1] and M. Nicklas[1,*]

[1]*Max-Planck Institute for Chemical Physics of Solids, Nöthnitzer Straße 40, 01187 Dresden, Germany*
[2]*Leibniz-Institut für Festkörper- und Werkstoffforschung IFW, Helmholtz Straße 20, 01171 Dresden, Germany*
[3]*ESRF, BP 220, F-38043 Grenoble Cedex 9, France*
[4]*Experimental Physics VI, Center for Electronic Correlations and Magnetism, Institute of Physics, University of Augsburg, 86135 Augsburg, Germany*

(Received 9 March 2017; published 28 November 2017)

A rapid and anisotropic modification of the Fermi-surface shape can be associated with abrupt changes in crystalline lattice geometry or in the magnetic state of a material. We show that such an electronic topological transition is at the basis of the formation of an unusual pressure-induced tetragonal ferromagnetic phase in $Fe_{1.08}Te$. Around 2 GPa, the orthorhombic and incommensurate antiferromagnetic ground state of $Fe_{1.08}Te$ is transformed upon increasing pressure into a tetragonal ferromagnetic state via a conventional first-order transition. On the other hand, an isostructural transition takes place from the paramagnetic high-temperature state into the ferromagnetic phase as a rare case of a "type-0" transformation with anisotropic properties. Electronic-structure calculations in combination with electrical resistivity, magnetization, and x-ray diffraction experiments show that the electronic system of $Fe_{1.08}Te$ is instable with respect to profound topological transitions that can drive fundamental changes of the lattice anisotropy and the associated magnetic order.

DOI: 10.1103/PhysRevLett.119.227003

The overwhelming majority of structural phase transitions in crystalline materials is associated with changes of the symmetry or modifications of atomic positions in the unit cell. At this time, only a very few systems are known to exhibit a symmetry-conserving or "isostructural" phase transition involving pronounced variations in the metric of the unit cell. These so-called type-0 transformations are first-order transitions for fundamental reasons [1,2]. The examples are driven by a diversity of mechanisms that change the internal state of the material without breaking crystalline symmetry, e.g., changes of coordination in complex framework lattices [3] or electronic transitions, including valence transitions [4–6], metal-insulator transitions [7], and other changes of the electronic structure [8].

Transformations involving spin order with magnetoelastic couplings can appear as isostructural transitions, although time-reversal symmetry is broken. If a transition is driven by magnetic ordering, then marked jumps of the lattice anisotropy are not expected in $3d$-electron systems, such as $Fe_{1+y}Te$. However, another type of transition with magnetoelastic coupling can be envisaged which is driven by a symmetry-conserving instability of the lattice. Such a "type-0" transition mode gives rise to magnetic ordering as a secondary effect. The resulting phase, an anisotropically deformed isostructural lattice with magnetic order as a by-product, is reached through a strongly discontinuous first-order transformation process. In metallic systems, abrupt changes in the unit-cell dimensions can be associated with modifications of the Fermi-surface (FS) topology, resulting in an electronic topological transition (ETT) [9–13]. We note that the changes in the FS topology discussed here are not related to the topologically protected surface states.

In this Letter, a thermal transition in $Fe_{1.08}Te$ under pressure is identified as an isostructural transition that is marked by a pronounced change of the axis ratio c/a in its tetragonal phase. This type-0 transformation is driven by lowering temperature, in contrast to the vast majority of type-0 transitions known in other materials, which are normally driven by a nonthermal control parameter, such as hydrostatic pressure. Furthermore, in $Fe_{1.08}Te$ the type-0 transformation triggers a ferromagnetic (FM) ordering as a secondary effect. Electronic-structure calculations explain the transition by a drastic change of the FS topology, as suggested originally by Lifshitz [14].

The nonsuperconducting parent compound of the Fe-based superconductors, $Fe_{1+y}Te$, has prompted the interests of the condensed matter community at large [15]. Bulk $Fe_{1+y}Te$ exhibits a plethora of structural and magnetic phase transitions as a function of excess Fe content (y), temperature (T) [16–21], and pressure (p) [22–27]. At low concentrations of $y \leq 0.11$, $Fe_{1+y}Te$ undergoes a structural and magnetic phase transition from a high-T tetragonal and paramagnetic (PM) semimetal to a low-T monoclinic antiferromagnet (AFM). For $y \geq 0.12$, an orthorhombic incommensurate AFM state is realized at low temperatures [16,18,28,29]. Similarly, applying pressure on a sample drives the system through a series of phase transitions that closely resemble those induced by

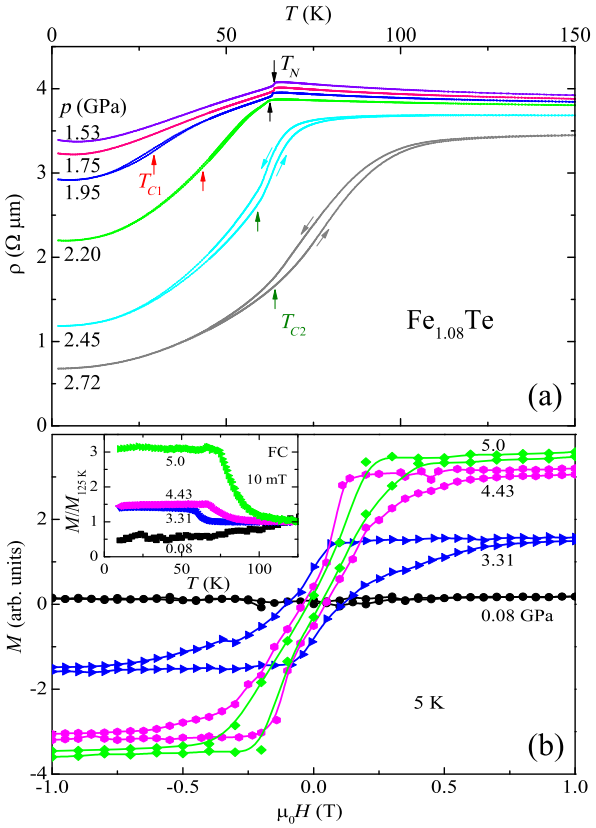

FIG. 1. (a) $\rho(T)$ data of $Fe_{1.08}Te$ for selected pressures collected upon cooling and heating as marked by arrows. T_N, T_{C1}, and T_{C2} are indicated. (b) $M(H)$ hysteresis loops of $Fe_{1.08}Te$ at 5 K and at different pressures. (Inset) Field-cooled (FC) $M(H)$ data for selected pressures.

excess Fe content [24]. One such transition, being completely unanticipated, is of particular interest: a pressure-induced FM phase transition at low temperatures [25,30–33]. This phase has not been observed at ambient pressure for samples of any level of Fe excess.

Details on the preparation of polycrystalline $Fe_{1.08}Te$ samples by a solid-state reaction and on the electrical resistivity, magnetization, and x-ray diffraction (XRD) experiments under pressure as well as on the density-functional theory based calculations can be found in the Supplemental Material [34].

The temperature dependence of the electrical resistivity ρ of $Fe_{1.08}Te$ taken in cooling and heating cycles for selected pressures $1.53\ \text{GPa} \leq p \leq 2.72\ \text{GPa}$ is displayed in Fig. 1(a). At a pressure of around 2.2 GPa, we observe a characteristic change in $\rho(T)$ in the paramagnetic phase at high temperatures. While $\rho(T)$ increases slightly upon lowering temperature at $p \leq 2.20$ GPa, indicating a semiconductinglike behavior, $\rho(T)$ decreases at higher pressures, as expected in a metal.

At 1.53 GPa, a small steplike feature in $\rho(T)$ around $T_N = 65$ K indicates the phase transition from a tetragonal PM to an orthorhombic incommensurate AFM phase [26]. This steplike feature is in contrast to the continuous anomaly observed at lower pressures. It does not show any thermal hysteresis, pointing to a second-order character of the phase transition. Upon further cooling, metallic behavior is observed down to 7 K, below which $\rho(T)$ exhibits a small upturn. The latter feature is less pronounced at higher pressures but remains visible up to 2.20 GPa. The height of the steplike feature marking T_N is suppressed upon increasing pressures. It is still clearly visible at 1.95 GPa, where a thermal hysteresis in $\rho(T)$, centered around 30 K and extending over a wide temperature range, is detected well below $T_N = 63$ K. The hysteresis is related to a first-order phase transition at $T_{C1} \approx 30$ K. Measurements of $\rho(T)$ in different magnetic fields (see the Supplemental Material [34]) give a first hint that T_{C1} is associated with a phase transition from the incommensurate AFM phase to a ferromagnetically ordered state at lower temperatures. A very weak anomaly in $\rho(T)$ at T_N still exists at 2.20 GPa. Increasing pressure drives $T_{C1}(p)$ rapidly toward higher temperatures. Concurrently, the temperature interval of the thermal hysteresis decreases, but it extends almost up to T_N. This observation suggests a competition between the FM and incommensurate AFM ordering.

For $p \gtrsim 2.4$ GPa, only a broad feature with a large thermal hysteresis remains in $\rho(T)$, signaling a first-order phase transition from the PM to the FM state at T_{C2} (T_{C2} is defined by the kink in the warming curve). Furthermore, the resistivity decreases monotonically toward the lowest temperatures. $T_{C2}(p)$ increases strongly with increasing pressure accompanied by an increase in the width of the thermal hysteresis. The positive field dependence of the anomaly at T_{C2} is consistent with a FM nature of the ordered state (see the Supplemental Material [34]).

At 5 K, the hysteresis in the magnetization $M(H)$ loops confirms the FM nature of the high-pressure phase [see Fig. 1(b)]. No signal can be resolved in the AFM phases at low pressures. Because of the large uncertainty in the determination of the sample mass, we cannot provide absolute values of the magnetization. However, this does not affect the relative changes between different pressures. Our finding is further supported by neutron diffraction data on $Fe_{1.141}Te$, which indicate that all Fe moments are oriented along the c axis in the pressure-induced FM phase [30]. The saturated high-field magnetization increases with increasing pressure, signifying a stabilization of ferromagnetism under pressure. $M(T)$ taken upon cooling in 10 mT shows a strong increase toward low temperatures upon entering the FM phase [inset of Fig. 1(b)]. The extracted transition temperatures $T_{C2}(p)$ are in good agreement with the ones obtained from $\rho(T)$.

The $T - p$ phase diagram in Fig. 2(a) summarizes the results of our $\rho(T)$ and $M(T)$ investigations and, additionally, includes the XRD data taken on $Fe_{1.08}Te$. One second-order (T_N) and two first-order (T_{C1} and T_{C2}) phase-transition lines meet at a multicritical point at $p_{MP} \approx 2.4$ GPa and

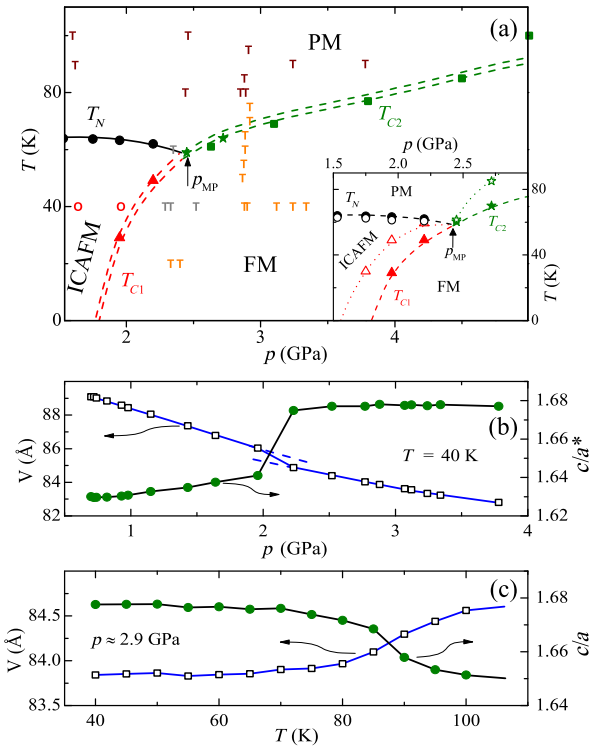

FIG. 2. (a) $T-p$ phase diagram for $Fe_{1.08}Te$. triangle, star, and circle mark the transition temperatures extracted from $\rho(T)$, and square that from $M(T)$. The letters T and O represent tetragonal and orthorhombic phases according to XRD measurements. The single line and the double lines indicate second-order and first-order phase transitions, respectively. (Inset) The $T-p$ phase diagram at zero field (solid symbols, dashed lines) and at 9 T (open symbols, dotted lines). ICAFM denotes incommensurate AFM. (b),(c) Unit-cell volume V (left axis) and c/a^* ratio (right axis) at 40 K as a function of pressure, and at ~2.9 GPa as a function of temperature, respectively.

$T_{\mathrm{MP}} \approx 58$ K. A field of 9 T suppresses T_N only weakly, but it strongly enhances T_{C1} and T_{C2}, except for the very vicinity of the multicritical point [Fig. 2(a), inset]. The strong increase in T_{C1} and T_{C2} is expected for a ferromagnet. We note that while, at 1.75 GPa in zero field, no T_{C1} anomaly in $\rho(T)$ is resolved down to 1.8 K, a field of 9 T induces FM ordering below $T_{C1}^{9\mathrm{T}} \approx 30$ K.

By entering the FM phase from the incommensurate AFM upon increasing pressure, the lattice symmetry changes from orthorhombic to tetragonal. The XRD data taken at 40 K upon increasing pressure indicate a broad two-phase region dominated by the tetragonal phase in a pressure window between 2.1 and 2.5 GPa consistent with the large hysteresis observed in the electrical resistivity. The transition from the orthorhombic-incommensurate AFM to the tetragonal-FM phase at T_{C1} is accompanied by a reduction of the unit-cell volume V and an increase in the ratio of the c- and a^*-axis lattice parameters [for orthorhombic and monoclinic symmetries $a^* = \frac{1}{2}(a+b)$]. At $T_{C1} = 40$ K we find a marked change in both V and the c/a^* ratio, by -0.6% and 2.1%,

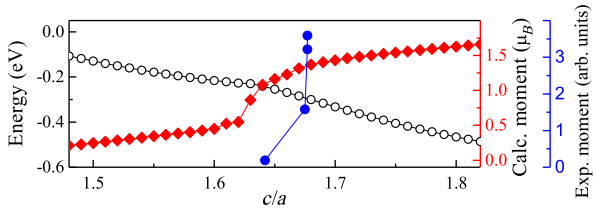

FIG. 3. Energy and Fe moment (calculated and experimental) as a function of the c/a ratio for stoichiometric FeTe ($Fe_{1.08}Te$). In the experimental data, p is an implicit parameter.

respectively, upon the transformation from the orthorhombic AFM to the tetragonal-FM state [see Fig. 2(b)]. This transformation connects two phases with different and unrelated magnetic symmetries, which explains why a classical first-order-type behavior with hysteresis is observed.

At T_{C2}, by contrast, the transformation from the high-temperature PM to the low-temperature FM state also takes place as a first-order process, evidenced by the large hysteresis observed in the $\rho(T)$ data, but without change of the tetragonal lattice symmetry. At this symmetry-conserving phase transition at T_{C2}, marked variations in V and the c/a ratio are again seen, e.g., -0.8% and 1.5% at ~2.9 GPa, respectively [see Fig. 2(c)]. This testifies that this phase transition is not driven by magnetic ordering. Rather, the marked change of the lattice aspect ratio and its volume suggests that the internal electronic structure of the material is fundamentally transformed when entering the FM state. The reason for the transformation, therefore, is not a symmetry breaking in the spin structure, but rather an isostructural instability of the tetragonal lattice. We note that the changes in V and the c/a ratio upon entering the tetragonal-FM phase are similar, independent of the path, i.e., upon entering from the orthorhombic-incommensurate AFM or from the tetragonal-PM phase. In the following we turn to electronic-structure calculations to track the FS evolution across the symmetry-conserving phase transition.

For simplicity, we have limited our band-structure analysis to the tetragonal phase and stoichiometric composition. The energetics and magnetic moments are analyzed as a function of the c/a ratio while we constrain the volume to that measured for 2.9 GPa (see the previous paragraph). First, we observe a salient feature in the total energy with an increasing c/a ratio (see Fig. 3): a non-monotonic flattening of the curve around $c/a \approx 1.6$, resulting in a shallow minimum. Upon further increase of the c/a ratio, the total energy then continues to decrease monotonically. Concomitantly, around $c/a \approx 1.6$, the Fe moment shows a sharp increase, strengthening from $0.4\mu_B$ to more than $1.5\mu_B$. Although the change in the total energy is subtle, the jump in the Fe moment is quite abrupt and can be construed as being emblematic of the first-order character of the symmetry-conserving phase transition, which is consistent with our experiments.

Second, we monitored the change in the electronic structure of FeTe. Collected in Fig. 4 are the FSs for

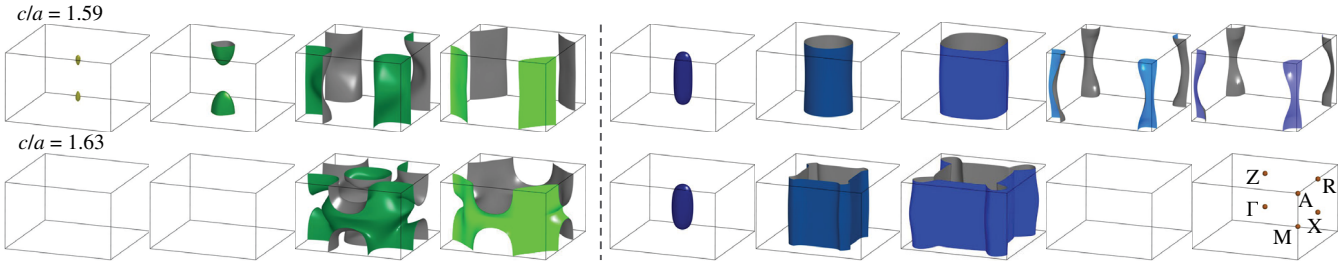

FIG. 4. Topological changes of the FS sheets for two closely spaced c/a ratios in FeTe. The left four FS sheets correspond to the spin-up channel (green), and the right five ones to the spin-down channel (blue). Upon increasing the c/a ratio by only 2.5%, four FS sheets (two in each spin channel) disappear, illustrative of an ETT.

two closely spaced c/a ratios adjoining the jump in Fig. 3. Upon increasing the c/a ratio from 1.59% by 2.5%, which is comparable to the experimentally observed increase at the symmetry-conserving transition, four FS sheets (two in each spin channel) rapidly reduce in volume and subsequently disappear. This is illustrative of the anticipated ETT, in the same vein as a Lifshitz transition [14]. We note that we find a similar change in the c/a^* ratio at the orthorhombic-incommensurate AFM to tetragonal-FM transition upon varying pressure.

Corresponding to the c/a variation, a pronounced narrow peak in the density of states (see the Supplemental Material [34]) jumps from below the Fermi level to above, thereby shifting the Fermi energy away from the van Hove–like singularity. The loss of charge carriers due to the disappearing FS sheets is more than compensated for by the remaining sheets, which increase significantly in volume, consistent with the electrical resistivity becoming more metallicklike at higher pressures. Hence, the combined changes in the topology of the FS, concomitant with the depopulation of the narrow density of states peak and the sharp increase of the Fe moment, demonstrate a Lifshitz ETT in the spin-split band structure of $Fe_{1.08}Te$ [8,14]. Lifshitz already demonstrated that ETTs can drive type-0 transitions [14], and it is known that electron-phonon coupling can exacerbate anisotropic inharmonic response and instability of the lattice [40]. However, the remarkable change of the c/a ratio in $Fe_{1.08}Te$ is unconventional and suggests that particular electron-phonon interactions exist in this system, so that the ETT results in an anisotropic lattice distortion. As we are observing a transition at finite temperature, its microscopic understanding should rely on the coupling of thermally smeared electronic states near singular Fermi-surface pieces to thermally excited acoustic phonons. Theoretically, such a strongly anisotropic effect in a $3d$-electron metallic system has not been anticipated; see the review in Ref. [41].

Phenomenologically, the first-order thermal PM-FM transition can be understood by considering the lattice strain, i.e., the change of the c/a ratio, as the order parameter, $\eta = e_{zz}$. It transforms as identity representation of the lattice space group. Coupled to the magnetization m, the Landau potential for this transition reads ($f = \alpha m^2 + \beta m^4 + A\eta^2 + B\eta^3 + C\eta^4 + d\eta m^2$), where the last (attractive) term, $d < 0$, encodes the unconventionally strong magnetoelastic coupling that relies on the ETT in the spin-split band structure. A first-order transition in the primary order parameter η is prompted by the cubic term B, and it can lead to a jumplike onset of magnetic order if $|d|$ is comparable to $\alpha > 0$, as in similar systems with coupled ordering modes [42,43]. This fundamental thermodynamic model describes all qualitative features and the strengths of the observed thermal transition in $Fe_{1.08}Te$ as a type 0 process driven by the lattice instability η. By contrast, a magnetically driven transition would have to reach $\alpha < 0$, which entails only a weak response of the lattice (details are in the Supplemental Material [34]).

Another important structural aspect aiding the ETT-induced FM state in $Fe_{1.08}Te$ is the anisotropic *enhancement* of the $c/a^{(*)}$ ratio under pressure. An anomalous expansion of the lattice parameters under pressure has been observed in various members of the Fe-based superconductors, but they tend to reduce relatively quickly afterwards. They include the realization of a collapsed state, wherein the c/a ratio is reduced considerably [44–48]. The formation of interlayer bonds is seen as a driving force for the collapsed state, which in turn becomes nonmagnetic [45]. By contrast, in $Fe_{1.08}Te$ the c/a ratio is *enhanced* in the FM state upon entering from the orthorhombic-incommensurate AFM phase or upon cooling from the tetragonal-PM one (Fig. 2). As seen in Fig. 3, such an increase in the c/a ratio is decisive in stabilizing the FM moment in $Fe_{1.08}Te$.

The formation of different magnetic structures due to an ETT is commonly observed in rare-earth containing metals (heavy-fermion systems) [49,50], wherein the localized moments of the rare-earth ions are interacting via the Ruderman-Kittel-Kasuya-Yosida (RKKY) mechanism [51]. Small changes in the FS topology of the conduction electrons which regulate the exchange mechanism can result in drastic changes of the magnetic properties. Dynamical mean-field theory studies on FeTe reported a mass enhancement of more than seven for the $3d_{xy}$ orbital, which is typical for heavy-fermion systems, and surmised that FeTe can promote an orbital-selective localization [39]. Another study, based on semiphenomenological models with coupled localized-itinerant moments in $Fe_{1+y}Te$, discussed the appearance of new magnetic phases by the y-dependent RKKY part of the interaction [52]. In our work, projecting out the $3d$

orbital character, we notice the FS sheets to be composed predominantly of the itinerant $3d_{xz/yz}$ and $3d_{x^2-y^2}$ orbitals (see the Supplemental Material [34]), while the $3d_{xy}$ orbital remains localized and away from the Fermi level. Consequently, the calculated rapid change in the FS topology, the sudden increase of the Fe moment, and the stabilization of the FM phase in $Fe_{1.08}Te$ bear some similarity to heavy-fermion materials in that the moments on the localized $3d_{xy}$ orbital are mediated by the other itinerant electrons. Thus, $Fe_{1.08}Te$ presents a rare example of an ETT-induced FM transition under pressure in a $3d$ system, wherein only a handful of examples (mostly containing rare-earth ions) exist in the literature [53–57].

Our results identify a topological transition of the Fermi surface in the (spin-split) electronic band structure of $Fe_{1+y}Te$ that leads to a coupled instability of the lattice geometry with magnetic ordering and explains its unconventional magnetostructural type-0 transformation in the thermal energy range at a pressure of a few gigapascals. The results demonstrate the subtle competition between various electronic degrees of freedom and the coupling to (the geometry of) the lattice as the relevant parameter to explain the existence of the many different phases in this Fe chalcogenide.

D. K. acknowledges funding from the Deutsche Forschungsgemeinschaft (DFG) within FOR 1346. U.S., S. W., and S. R. acknowledge support from the DFG within SPP 1458.

*nicklas@cpfs.mpg.de

[1] R. A. Cowley, Acoustic phonon instabilities and structural phase transitions, Phys. Rev. B **13**, 4877 (1976).
[2] A. G. Christy, Isosymmetric structural phase transitions: Phenomenology and examples, Acta Crystallogr. Sect. B **51**, 753 (1995).
[3] D. Saha, R. Ranjan, D. Swain, C. Narayana, and T. N. Guru Row, An unusual temperature induced isostructural phase transition in a scheelite $Li_{0.5}Ce_{0.5}MnO_4$, Dalton Trans. **42**, 7672 (2013).
[4] A. W. Larson and T.-Y. Tang, Concerning the high pressure allotropic modification of cerium, Phys. Rev. **76**, 301 (1949).
[5] N. Lanatà, Y.-X. Yao, C.-Z. Wang, K.-M. Ho, J. Schmalian, K. Haule, and G. Kotliar, γ-α Isostructural Transition in Cerium, Phys. Rev. Lett. **111**, 196801 (2013).
[6] J. L. Sarrao, C. D. Immer, C. L. Benton, Z. Fisk, J. M. Lawrence, D. Mandrus, and J. D. Thompson, Evolution from first-order valence transition to heavy-fermion behavior in $YbIn_{1-x}Ag_xCu_4$, Phys. Rev. B **54**, 12207 (1996).
[7] Y. Akahama, H. Kawamura, D. Häusermann, M. Hanfland, and O. Shimomura, New High-Pressure Structural Transition of Oxygen at 96 GPa Associated with Metallization in a Molecular Solid, Phys. Rev. Lett. **74**, 4690 (1995).
[8] H. Rosner, D. Koudela, U. Schwarz, A. Handstein, M. Hanfland, I. Opahle, K. Koepernik, M. D. Kuz'min, K. H. Müller, J. A. Mydosh, and M. Richter, Magnetoelastic lattice collapse in YCo_5, Nat. Phys. **2**, 469 (2006).
[9] D. L. Novikov, M. I. Katsnelson, A. V. Trefilov, A. J. Freeman, N. E. Christensen, A. Svane, and C. O. Rodriguez, Anisotropy of thermal expansion and electronic topological transitions in Zn and Cd under pressure, Phys. Rev. B **59**, 4557 (1999).
[10] C. Liu, T. Kondo, R. M. Fernandes, E. D. Palczewski, A. D. Mun, N. Ni, A. N. Thaler, A. Bostwick, E. Rotenberg, J. Schmalian, S. L. Bud'ko, P. C. Canfield, and A. Kaminski, Evidence for a Lifshitz transition in electron-doped iron arsenic superconductors at the onset of superconductivity, Nat. Phys. **6**, 419 (2010).
[11] K. Glazyrin *et al.*, Importance of Correlation Effects in hcp Iron Revealed by a Pressure-Induced Electronic Topological Transition, Phys. Rev. Lett. **110**, 117206 (2013).
[12] F. J. Manjón, R. Vilaplana, O. Gomis, E. Pérez-González, D. Santamaría-Pérez, V. Marín-Borrás, A. Segura, J. González, P. Rodríguez-Hernández, A. Muñoz, C. Drasar, V. Kucek, and V. Muñoz Sanjos, High-pressure studies of topological insulators Bi_2Se_3, Bi_2Te_3, and Sb_2Te_3, Phys. Status Solidi B **250**, 669 (2013).
[13] L. Dubrovinsky, N. Dubrovinskaia, E. Bykova, M. Bykov, V. Prakapenka, C. Prescher, K. Glazyrin, H.-P. Liermann, M. Hanfland, M. Ekholm, Q. Feng, L. V. Pourovskii, M. I. Katsnelson, J. M. Wills, and I. A. Abrikosov, The most incompressible metal osmium at static pressures above 750 gigapascals, Nature (London) **525**, 226 (2015).
[14] I. M. Lifshitz, Anomalies of electron characteristics of a metal in the high pressure region, Zh. Eksp. Teor. Fiz. **38**, 1569 (1960) [Sov. Phys. JETP **11**, 1130 (1960)].
[15] K. Deguchi, Y. Takano, and Y. Mizuguchi, Physics and chemistry of layered chalcogenide superconductors, Sci. Technol. Adv. Mater. **13**, 054303 (2012).
[16] E. E. Rodriguez, C. Stock, P. Zajdel, K. L. Krycka, C. F. Majkrzak, P. Zavalij, and M. A. Green, Magnetic-crystallographic phase diagram of the superconducting parent compound $Fe_{1+x}Te$, Phys. Rev. B **84**, 064403 (2011).
[17] I. A. Zaliznyak, Z. J. Xu, J. S. Wen, J. M. Tranquada, G. D. Gu, V. Solovyov, V. N. Glazkov, A. I. Zheludev, V. O. Garlea, and M. B. Stone, Continuous magnetic and structural phase transitions in $Fe_{1+y}Te$, Phys. Rev. B **85**, 085105 (2012).
[18] C. Koz, S. Rößler, A. A. Tsirlin, S. Wirth, and U. Schwarz, Low-temperature phase diagram of $Fe_{1+y}Te$ studied using x-ray diffraction, Phys. Rev. B **88**, 094509 (2013).
[19] E. E. Rodriguez, D. A. Sokolov, C. Stock, M. A. Green, O. Sobolev, J. A. Rodriguez-Rivera, H. Cao, and A. Daoud-Aladine, Magnetic and structural properties near the Lifshitz point in $Fe_{1+x}Te$, Phys. Rev. B **88**, 165110 (2013).
[20] T. Machida, D. Morohoshi, K. Takimoto, H. Nakamura, H. Takeya, T. Mochiku, S. Ooi, Y. Mizuguchi, Y. Takano, K. Hirata, and H. Sakata, Effect of excess Fe on magnetic properties and crystallographic phases in $Fe_{1+\delta}Te$, Physica (Amsterdam) **484C**, 19 (2013).
[21] D. Cherian, S. Rößler, C. Koz, A. A. Tsirlin, U. Schwarz, S. Wirth, and S. Elizabeth, Structural and thermodynamic properties of $Fe_{1.12}Te$ with multiple phase transitions, J. Appl. Phys. **115**, 123912 (2014).

[22] H. Okada, H. Takahashi, Y. Mizuguchi, Y. Takano, and H. Takahashi, Successive phase transitions under high pressure in $FeTe_{0.92}$, J. Phys. Soc. Jpn. **78**, 083709 (2009).

[23] H. Takahashi, H. Okada, H. Takahashi, Y. Mizuguchi, and Y. Takano, Electrical resistivity measurements under high pressure for $FeTe_{0.92}$, J. Phys. Conf. Ser. **200**, 012196 (2010).

[24] C. Koz, S. Rößler, A. A. Tsirlin, D. Kasinathan, C. Börrnert, M. Hanfland, H. Rosner, S. Wirth, and U. Schwarz, Pressure-induced successive structural transitions and high-pressure tetragonal phase of $Fe_{1.08}Te$, Phys. Rev. B **86**, 094505 (2012).

[25] M. Bendele, A. Maisuradze, B. Roessli, S. N. Gvasaliya, E. Pomjakushina, S. Weyeneth, K. Conder, H. Keller, and R. Khasanov, Pressure-induced ferromagnetism in antiferromagnetic $Fe_{1.03}Te$, Phys. Rev. B **87**, 060409(R) (2013).

[26] J. E. Jørgensen and D. Sheptyakov, Magnetic ordering in $Fe_{1.087}Te$ under pressure, Eur. Phys. J. B **86**, 18 (2013).

[27] J. E. Jørgensen and T. C. Hansen, Pressure-induced successive magnetic and structural phase transitions in $Fe_{1.087}Te$, Eur. Phys. J. B **88**, 119 (2015).

[28] Wei Bao, Y. Qiu, Q. Huang, M. A. Green, P. Zajdel, M. R. Fitzsimmons, M. Zhernenkov, S. Chang, Minghu Fang, B. Qian, E. K. Vehstedt, Jinhu Yang, H. M. Pham, L. Spinu, and Z. Q. Mao, Tunable $(\delta\pi, \delta\pi)$-Type Antiferromagnetic Order in α-Fe(Te, Se) Superconductors, Phys. Rev. Lett. **102**, 247001 (2009).

[29] Ph. Materne, C. Koz, U. K. Rößler, M. Doerr, T. Goltz, H. H. Klauss, U. Schwarz, S. Wirth, and S. Rößler, Solitonic Spin-Liquid State due to the Violation of the Lifshitz Condition in $Fe_{1+y}Te$, Phys. Rev. Lett. **115**, 177203 (2015).

[30] J.-E. Jørgensen and T. H. Hansen, Magnetic-crystallographic p, T-phase diagram of $Fe_{1.141}Te$: A high-pressure neutron diffraction study, Phys. Status Solidi B **253**, 2257 (2016).

[31] A. V. Fedorchenko, G. E. Grechnev, V. A. Desnenko, A. S. Panfilov, S. L. Gnatchenko, V. Tsurkan, J. Deisenhofer, A. Loidl, O. S. Volkova, and A. N. Vasiliev, Pressure effects on the magnetic susceptibility of $FeTe_x$ $(x \simeq 1.0)$, J. Phys. Condens. Matter **23**, 325701 (2011).

[32] M. Monni, F. Bernardini, G. Profeta, and S. Massidda, Theoretical investigation of FeTe magnetic ordering under hydrostatic pressure, Phys. Rev. B **87**, 094516 (2013).

[33] A. Ciechan, M. J. Winiarski, and M. Samsel-Czekała, Magnetic phase transitions and superconductivity in strained FeTe, J. Phys. Condens. Matter **26**, 025702 (2014).

[34] See Supplemental Material at http://link.aps.org/supplemental/10.1103/PhysRevLett.119.227003, which includes Refs. [24, 35–39], for additional information on (a) the sample growth and characterization, (b) the methods, (c) the electrical resistivity in magnetic fields, (d) the density functional theory calculations, and (e) the analysis within Landau theory.

[35] S. Rößler, C. Koz, S. Wirth, and U. Schwarz, Synthesis, phase stability, structural, and physical properties of 11-type iron chalcogenides, Phys. Status Solidi B **254**, 1600149 (2017).

[36] K. Koepernik and H. Eschrig, Full-potential nonorthogonal local-orbital minimum-basis band-structure scheme, Phys. Rev. B **59**, 1743 (1999).

[37] J. C. Tolédano and P. Tolédano, *The Landau Theory of Phase Transitions* (World Scientific, Singapore, 1987).

[38] A. I. Larkin and S. A. Pikin, On phase transitions of the first order resembling those of the second order, Zh. Eksp. Teor. Fiz. **56**, 1664 (1969) [Sov. Phys. JETP **29**, 891 (1969)].

[39] Z. P. Yin, K. Haule, and G. Kotliar, Kinetic frustration and the nature of the magnetic and paramagnetic states in iron pnictides and iron chalcogenides, Nat. Mater. **10**, 932 (2010).

[40] L. Dagens and C. Lopez-Rios, Thermodynamic properties of a metal near a Fermi surface topological transition: The anomalous electron-phonon interaction contribution, J. Phys. F **9**, 2195 (1979).

[41] Y. M. Blanter, M. I. Kaganov, A. V. Pantsulaya, and A. A. Varlamov, The theory of electronic topological transitions, Phys. Rep. **245**, 159 (1994).

[42] J. Holakovský, A new type of the ferroelectric phase transition, Phys. Status Solidi B **56**, 615 (1973).

[43] E. K. H. Salje and M. A. Carpenter, Linear-quadratic order parameter coupling and multiferroic phase transitions, J. Phys. Condens. Matter **23**, 462202 (2011).

[44] D. Kasinathan, A. Ormeci, K. Koch, U. Burkhardt, W. Schnelle, A. Leithe-Jasper, and H. Rosner, AFe_2As_2 (A = Ca, Sr, Ba, Eu) and $SrFe_{2-x}TM_xAs_2$ (TM = Mn, Co, Ni): Crystal structure, charge doping, magnetism and superconductivity, New J. Phys. **11**, 025023 (2009).

[45] D. Kasinathan, M. Schmitt, K. Koepernik, A. Ormeci, K. Meier, U. Schwarz, M. Hanfland, C. Geibel, Y. Grin, A. Leithe-Jasper, and H. Rosner, Symmetry-preserving lattice collapse in tetragonal $SrFe_{2-x}Ru_xAs_2$ $(x = 0, 0.2)$: A combined experimental and theoretical study, Phys. Rev. B **84**, 054509 (2011).

[46] C. W. Chu and B. Lorenz, High pressure studies on Fe-pnictide superconductors, Physica (Amsterdam) **469C**, 385 (2009).

[47] E. Gati, S. Köhler, D. Guterding, B. Wolf, S. Knöner, S. Ran, S. L. Bud'ko, P. C. Canfield, and M. Lang, Hydrostatic-pressure tuning of magnetic, nonmagnetic, and superconducting states in annealed $Ca(Fe_{1-x}Co_x)_2As_2$, Phys. Rev. B **86**, 220511(R) (2012).

[48] D. Guterding, S. Backes, H. O. Jeschke, and R. Valenti, Origin of the superconducting state in the collapsed tetragonal phase of KFe_2As_2, Phys. Rev. B **91**, 140503 (R) (2015).

[49] C. W. Chu, T. F. Smith, and W. E. Gardner, Study of Fermi-surface topology changes in rhenium and dilute Re solid solutions from T_c measurements at high pressure, Phys. Rev. B **1**, 214 (1970).

[50] A.Vl. Andrianov, Electronic topological transition of the Lifshitz type and complex magnetic structures in heavy rare-earth metals, Low Temp. Phys. **40**, 323 (2014).

[51] J. Jensen and A. R. Mackintosh, *Rare Earth Magnetism* (Clarendon Press, Oxford, 1991).

[52] S. Ducatman, R. M. Fernandes, and N. B. Perkins, Theory of the evolution of magnetic order in $Fe_{1+y}Te$ compounds with increasing interstitial iron, Phys. Rev. B **90**, 165123 (2014).

[53] H. Kadomatsu, H. Tanaka, M. Kurisu, and H. Fujiwara, Kondo state and pressure-induced ferromagnetism in CeZn, Phys. Rev. B **33**, 4799 (1986).

[54] R. Hauser, E. Bauer, E. Gratz, T. Häufler, G. Hilscher, and G. Wiesinger, Pressure dependence of the magnetic order in RMn_2 (R = rare earth), Phys. Rev. B **50**, 13493 (1994).

[55] M. Ishizuka, Y. Kai, R. Akimoto, M. Kobayashi, K. Amaya, and S. Endo, Pressure-induced ferromagnetism in EuTe, J. Magn. Magn. Mater. **166**, 211 (1997).

[56] F. Nakamura, Y. Senoo, T. Goko, M. Ito, T. Suzuki, S. Nakatsuji, H. Fukazawa, Y. Maeno, P. Alireza, and S. R. Julian, Pressure-induced ferromagnetic metal for a Mott insulator Ca_2RuO_4, Physica (Amsterdam) **329B–333B**, 803 (2003).

[57] N. Tateiwa, T. D. Matsuda, Y. Haga, and Z. Fisk, Pressure-induced ferromagnetism with strong Ising-type anisotropy in $YbCu_2Si_2$, Phys. Rev. B **89**, 035127 (2014).